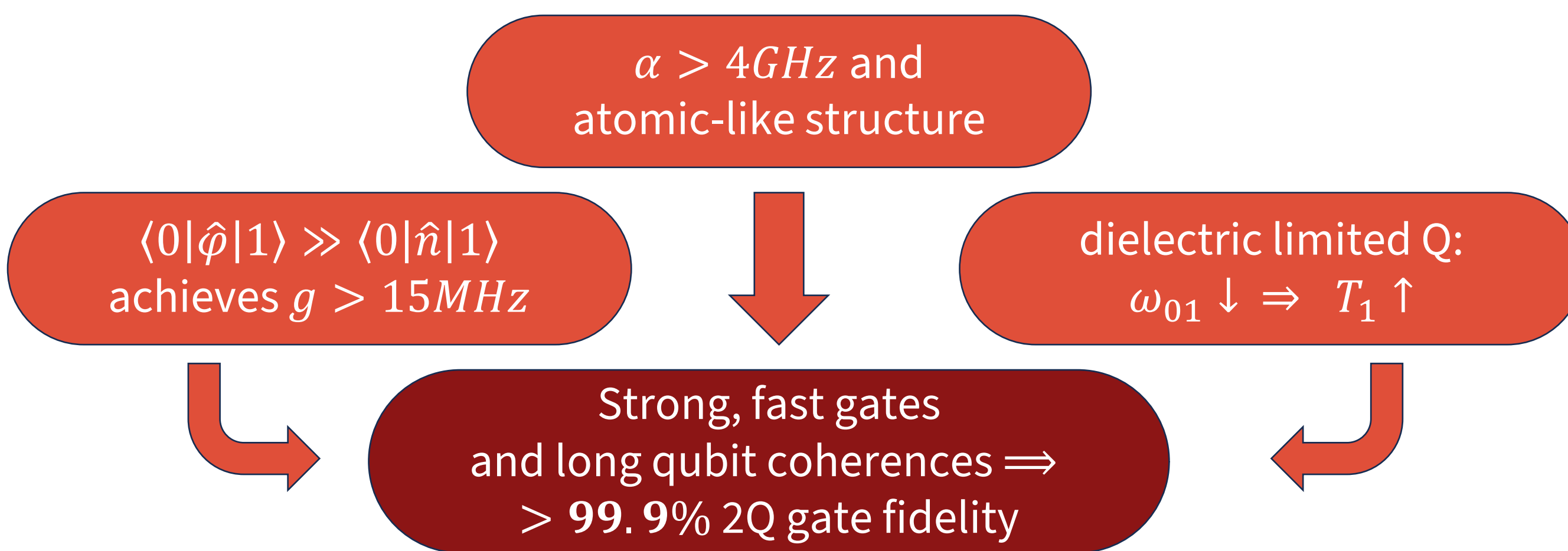
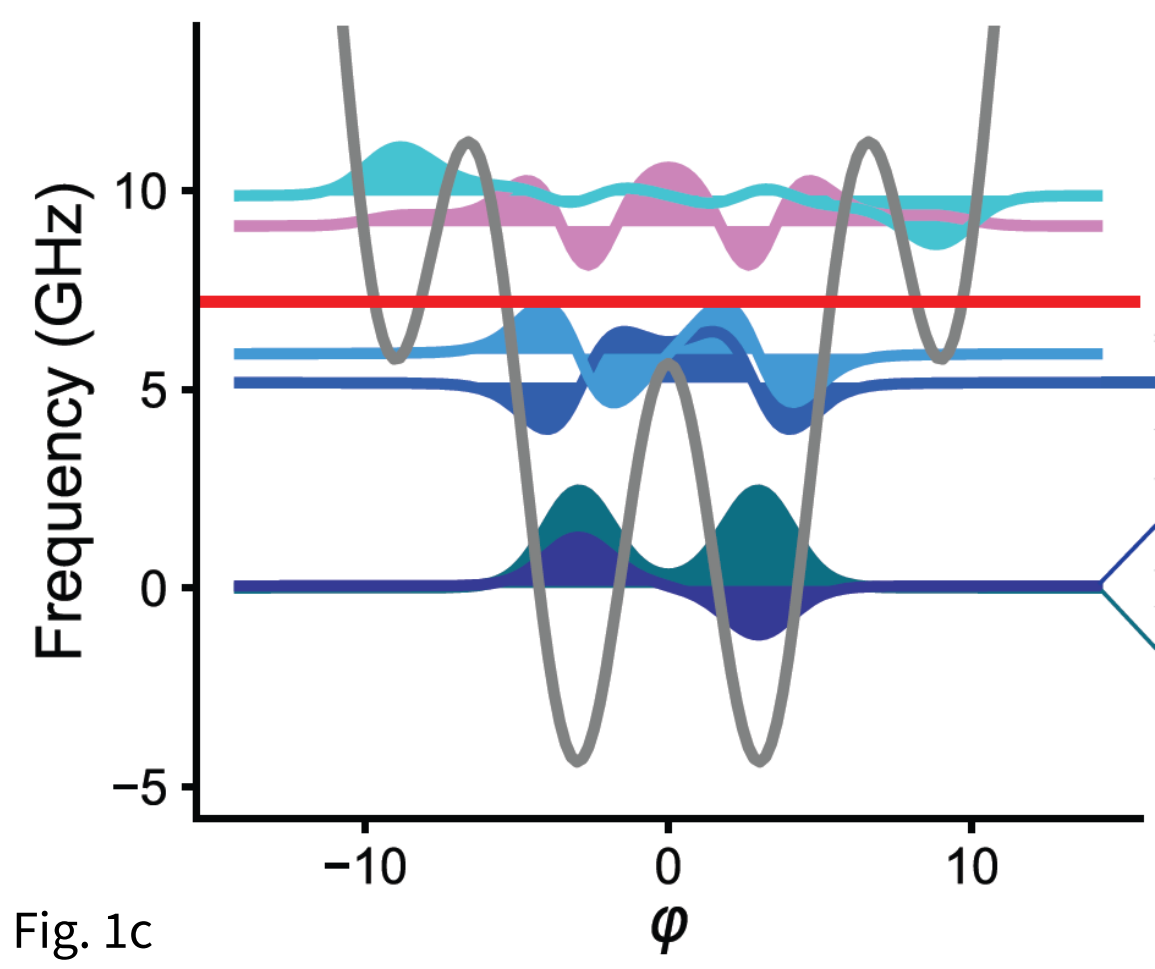


Why inductively coupled fluxonium?



2Q device Hamiltonians

$$\mathcal{H}_f = -4E_C \frac{d^2}{d\phi^2} - E_J \cos(\phi) + \frac{1}{2} E_L \left(\phi + 2\pi \frac{\Phi_{\text{ext}}}{\Phi_0} \right)^2$$



- Each fluxonium is capacitively shunted (small E_C), resulting in low $f < 100\text{MHz}$
- Although resonator detuning is $\Delta \sim 6\text{GHz}$, $X \sim 0.7\text{MHz}$ via coupling to plasmon levels

	qubit a	qubit b
f_{10} (GHz)	0.0618	0.0484
α (GHz)	4.41	5.06
T_1 (μs)	180	300
T_2^* (μs)	150	200
T_{2e} (μs)	250	300

Tab. S1

$$\mathcal{H}_{\text{eff}} = - \sum_{\mu=a,b} \left(\frac{\omega_{\mu}^{\mu}}{2} \sigma_z^{\mu} + \Omega_{\mu} \sigma_x^{\mu} \right) + J \sigma_x^a \sigma_x^b + \xi \sigma_z^a \sigma_z^b$$

\mathcal{H}_{eff} is found via perturbation theory near half-integer flux, where:

- ω_{μ} are dressed qubit freqs, incl. coupler-induced Lamb shifts
- $\Omega_{\mu}(\Phi_{\text{ext}}^{\mu}, \Phi_{\text{ext}}^C)$ executes single-qubit gates
- $J(\Phi_{\text{ext}}^A, \Phi_{\text{ext}}^B, \Phi_{\text{ext}}^C)$ gives the desired XX coupling; tunable to ~ 0
- ξ is an unwanted ZZ coupling, but is suppressed to be $< 3\text{kHz}$

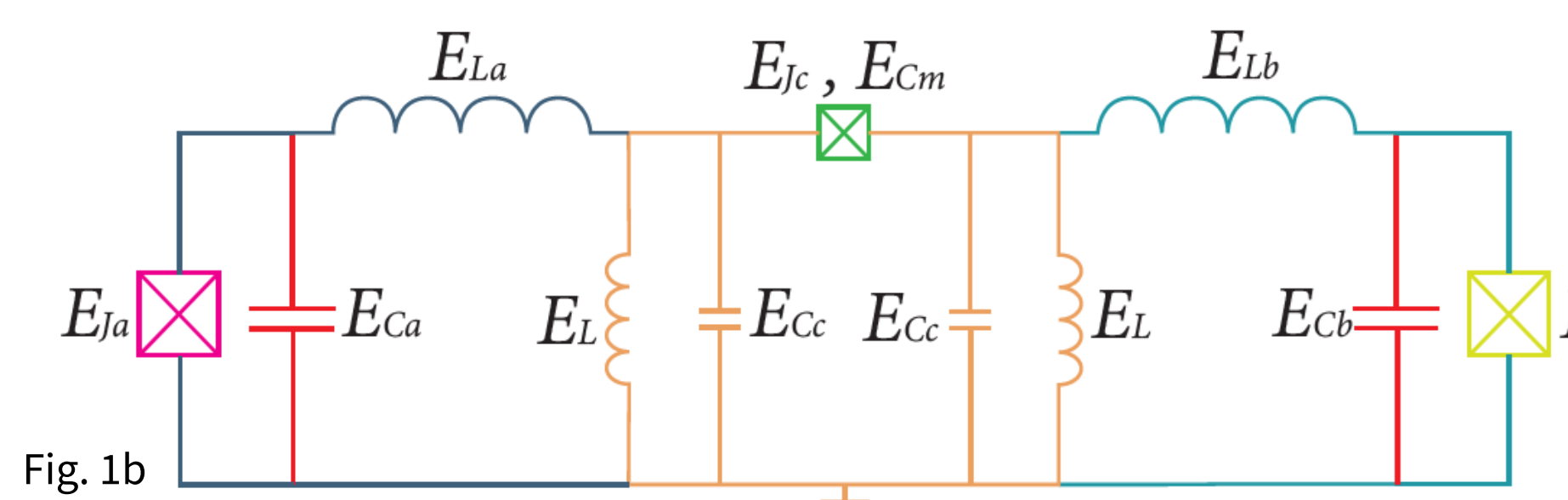
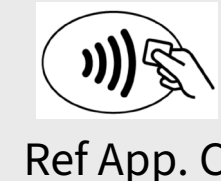
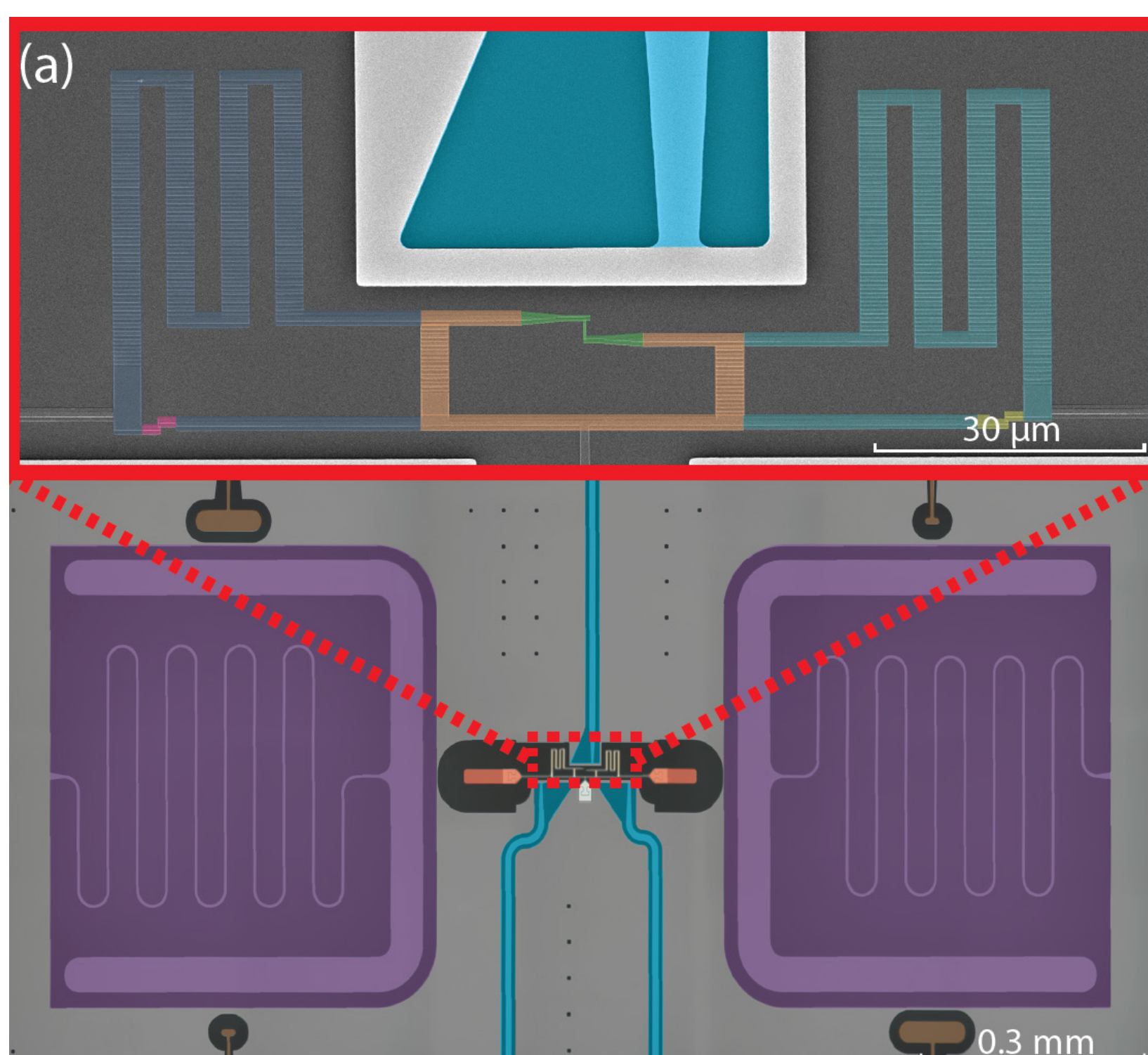


Fig. 1b

- Shared tunable inductor creates a $\varphi_A \varphi_B$ term

- In computational basis (via Schrieffer-Wolff): $\sigma_x^a \sigma_x^b$ [2]



- False colors correspond to circuit elements (above)
- Tantalum base metal (200nm) on sapphire substrate (430 μm), with aluminum junctions (70nm/90nm)
- Kinetic inductance realized by a chain of 238 Josephson junctions
- Galvanic connection between qubits and coupler is realized by a shared JJ chain, with 36 junctions

Fig. 1a

Tuning 2Q entangling gates ($\sqrt{b\text{SWAP}}$)

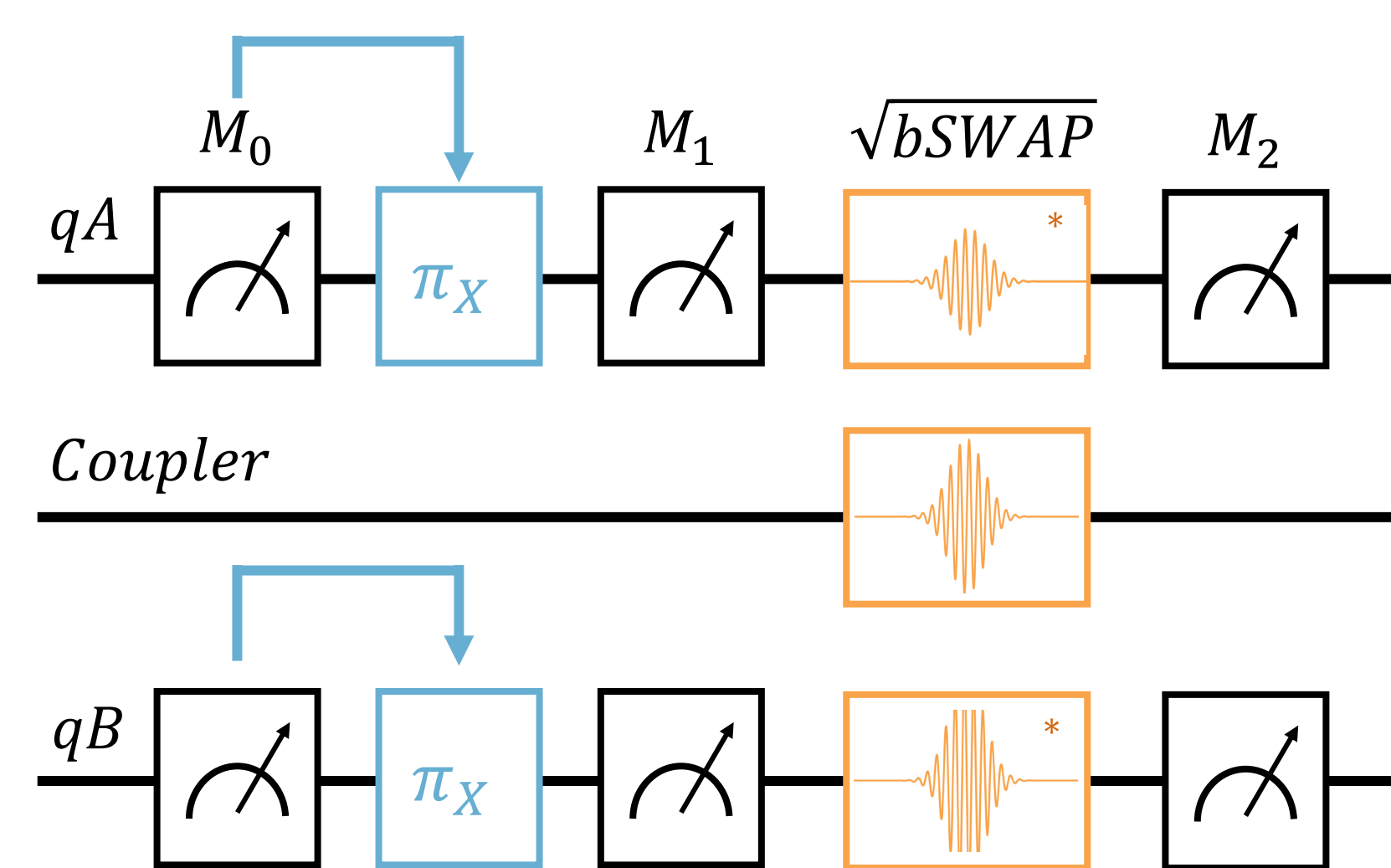
$$\sqrt{b\text{SWAP}} = \begin{pmatrix} 1/\sqrt{2} & 0 & 0 & i/\sqrt{2} \\ 0 & 1 & 0 & 0 \\ 0 & 0 & 1 & 0 \\ i/\sqrt{2} & 0 & 0 & 1/\sqrt{2} \end{pmatrix}$$

$$J(\Phi_{\text{ext}}^A, \Phi_{\text{ext}}^B, \Phi_{\text{ext}}^C) \sigma_x^A \sigma_x^B \Rightarrow A \sin(\omega_d t) [\cos(\omega_{\pm} t) \Sigma_x^{\pm} + \sin(\omega_{\pm} t) \Sigma_y^{\pm}] \text{ (interaction frame)}$$

$$\Rightarrow A [\sin(2\omega_{\pm} t) \Sigma_x^{\pm} + \cos(2\omega_{\pm} t) \Sigma_y^{\pm}] \text{ (RWA: } \omega_d = \omega_A + \omega_B)$$

$$\Rightarrow \sqrt{\phi_b \text{SWAP}} (\phi \propto t) [2]$$

Pulse sequence w/ active reset



Correlated oscillations between $|00\rangle \leftrightarrow |11\rangle$

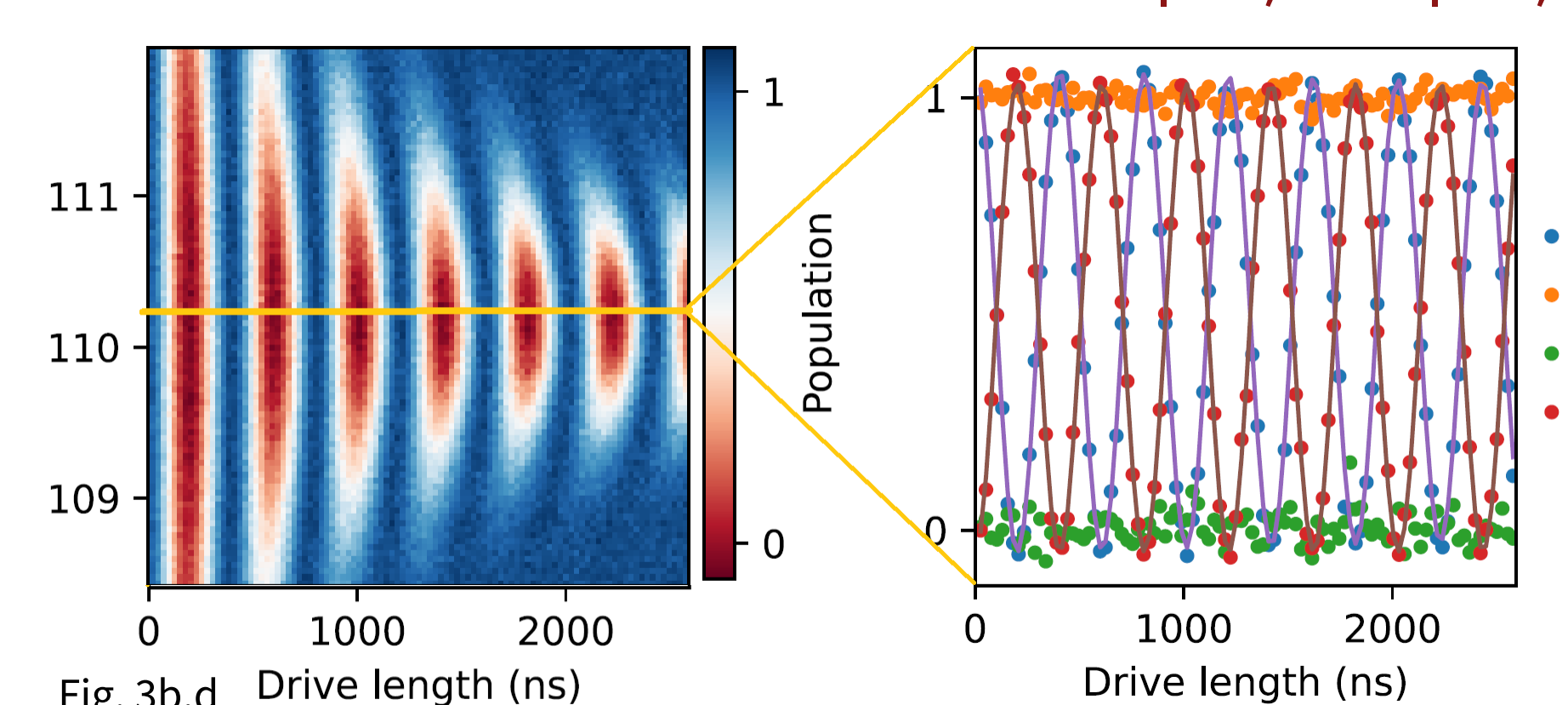


Fig. 3b,d Drive amplitude: $A = 0.011 \Phi_0$ Time for one full oscillation: 400ns (2.5MHz)

Device measurement and characterization

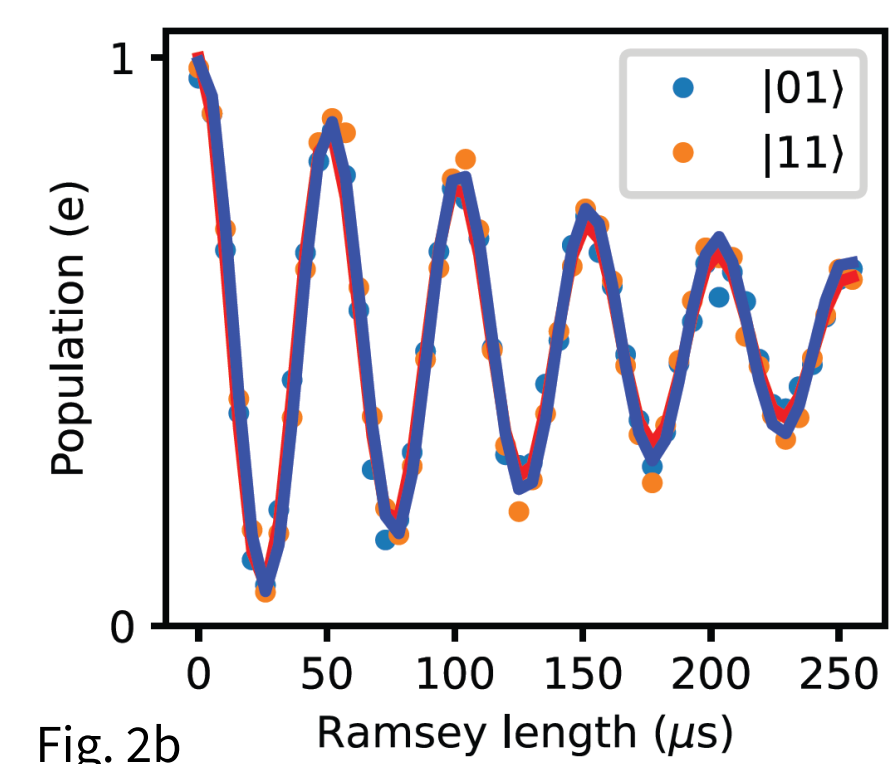


Fig. 2b

- Ramsey exp. of qB at $\Phi_{\text{ext}}^C \sim 0.3$, the "off position"
- ZZ is found via the freq. diff ($f_{11} - f_{10}$) - ($f_{01} - f_{00}$) and is measured to be $< 100\text{Hz}$

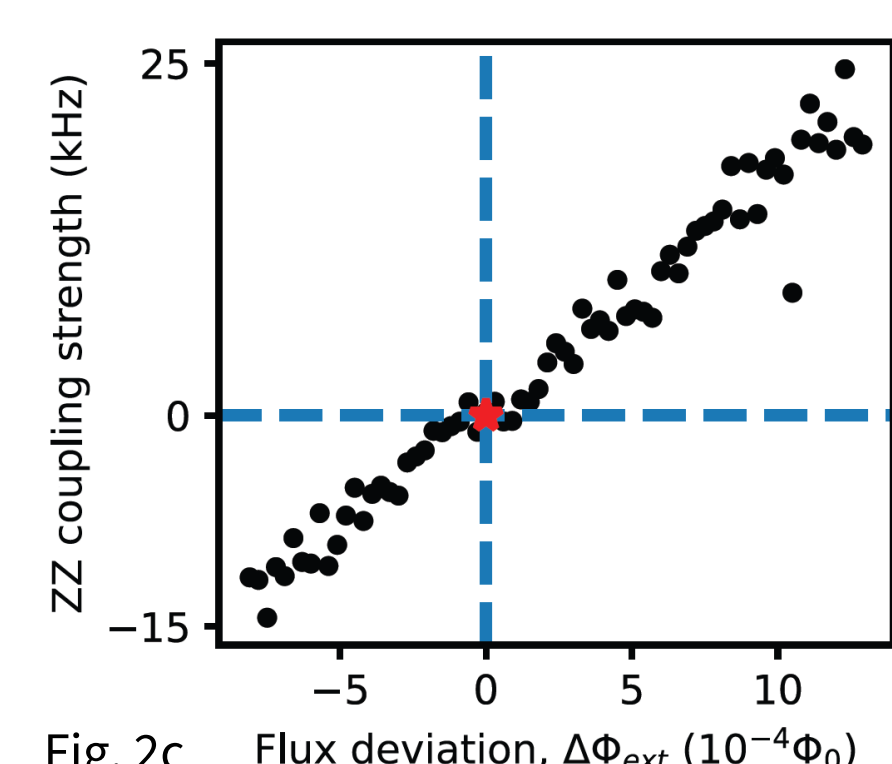


Fig. 2c

- Measured ZZ when tuning away from the "sweet spot contour"
- Used as an indicator for calibrating the "off position"

XX, ZZ as function of Φ_{ext}^C (sweet spot contour)

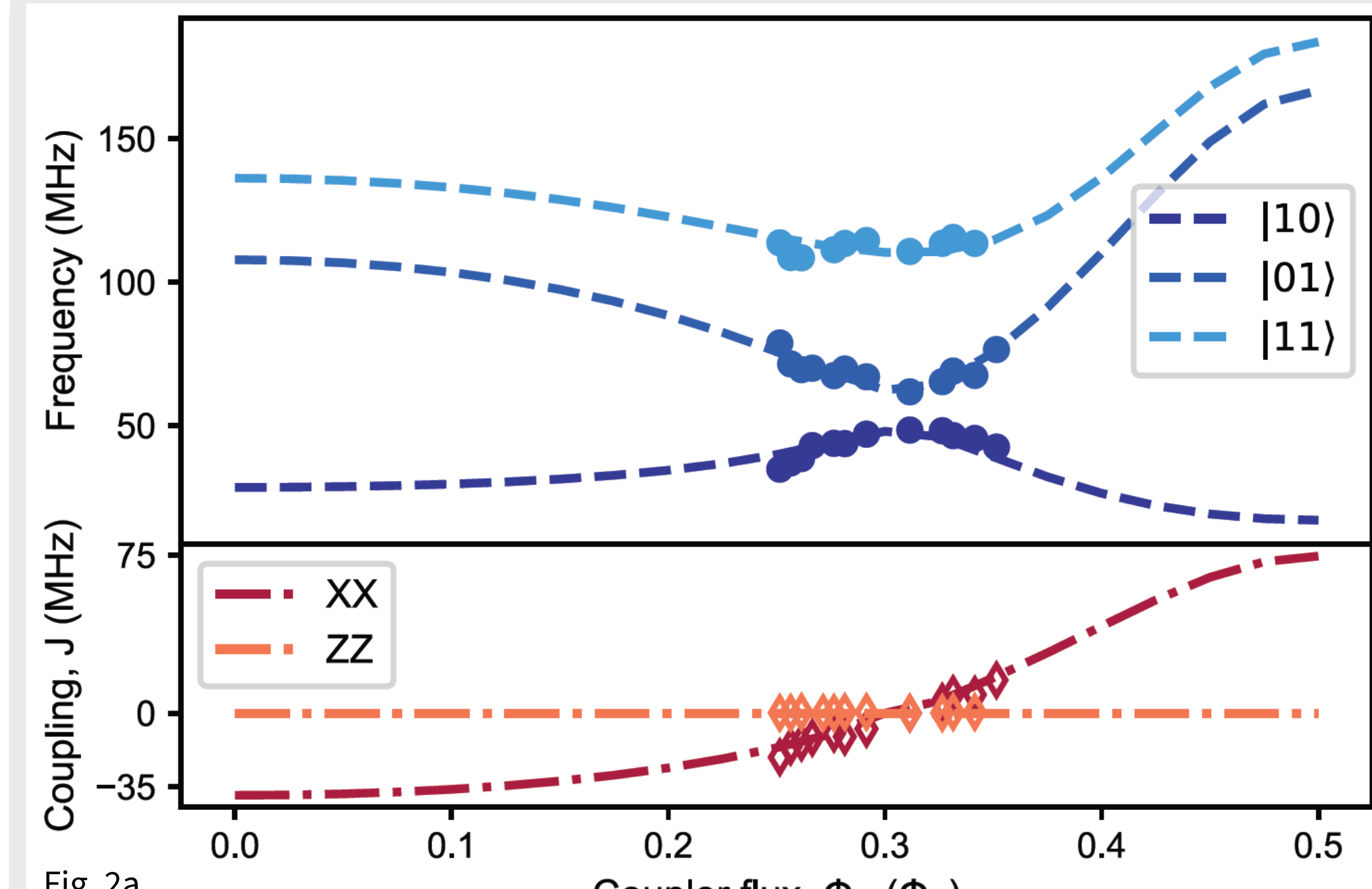


Fig. 2a

- Dots: measured qubit frequencies at various coupler flux
- Diamonds: measured XX and ZZ coupling strengths
- Dashed lines: theory curves using extracted qubit params
- ZZ coupling strength $< 3\text{kHz}$ across entire measured range
- XX strength measured between -20 to $+15\text{MHz}$, with on-off contrast $> 10^5$

Qubit parameters, determined by fitting to plasmon spectroscopy lines via **scqubits**

	qubit a	qubit b	coupler φ_-	coupler φ_+
E_J (GHz)	5.65	4.88	4.246	
E_C (GHz)	0.95	0.905	8	12
E_L (GHz)	0.292	0.286	3.52	3.52

qB spectroscopy ($\Phi_{\text{ext}}^C = \Phi_{\text{ext}}^B = 0$)

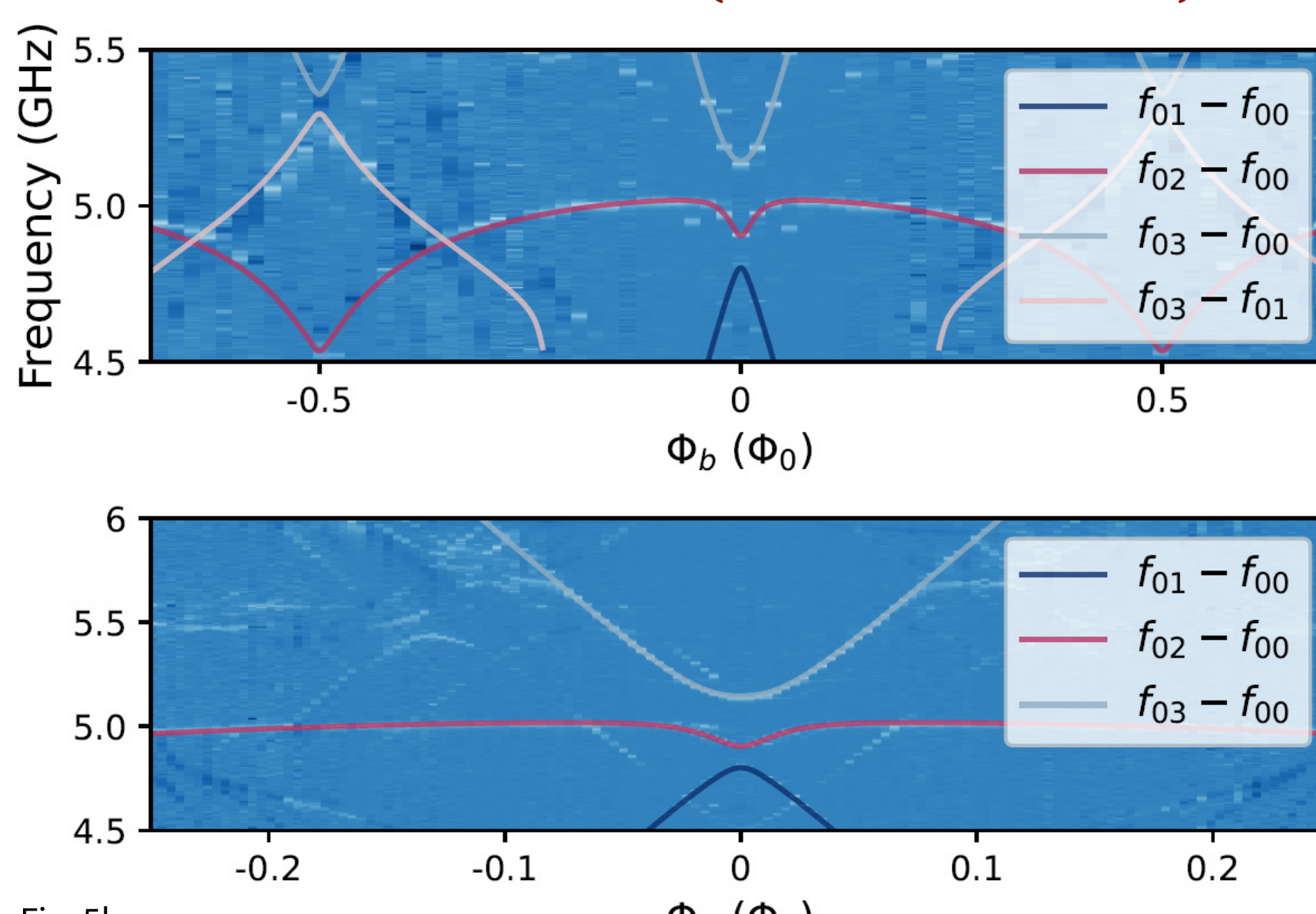
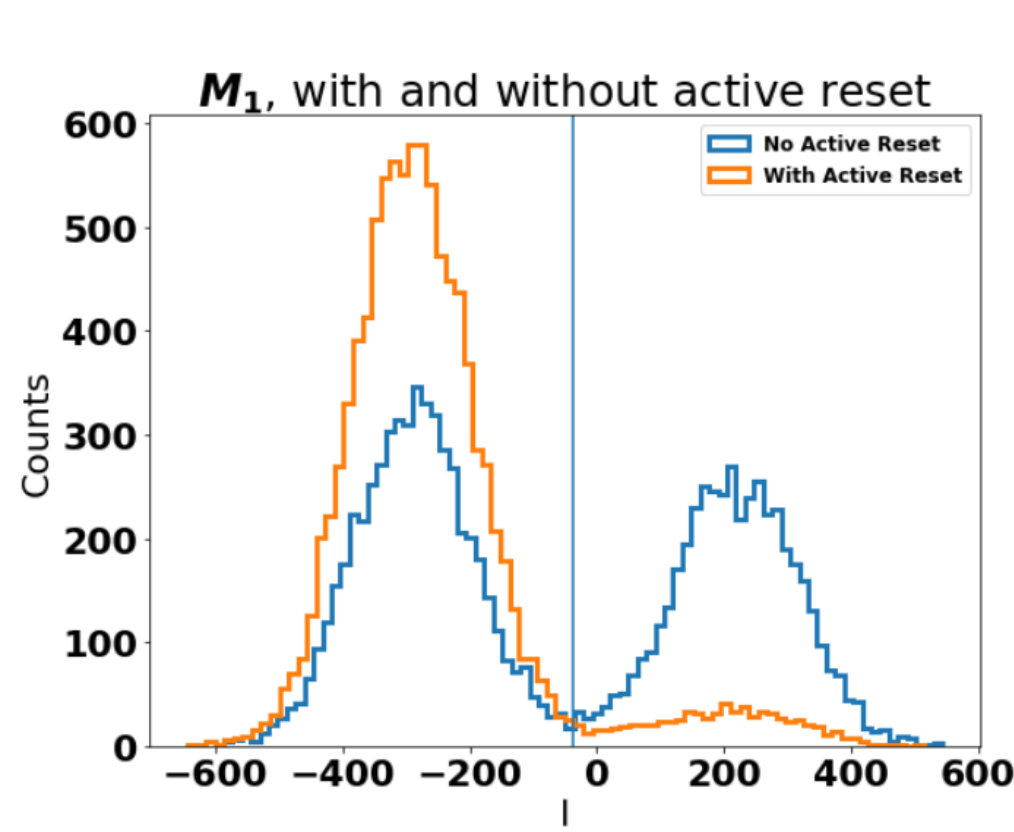
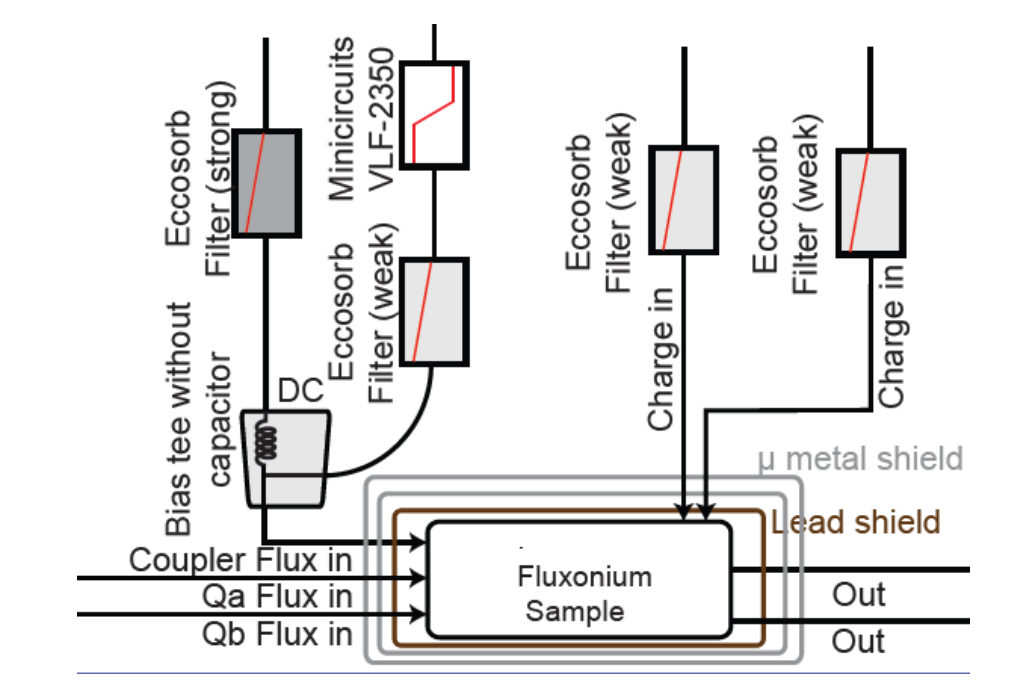


Fig. 5b,c



- Filter qubit lines using Eccosorb IR & K&L lowpass filters
- The qubit's Boltzmann temperature ($hf/k_B = 2.8\text{mK}$) is lower than its environment, measured to be $\sim 50\text{mK}$
- Active reset and postselection is necessary for initializing the qubit
- Realized using the QICK firmware [3] on a Xilinx ZCU111 rfSoc

Phase & crosstalk calibrations

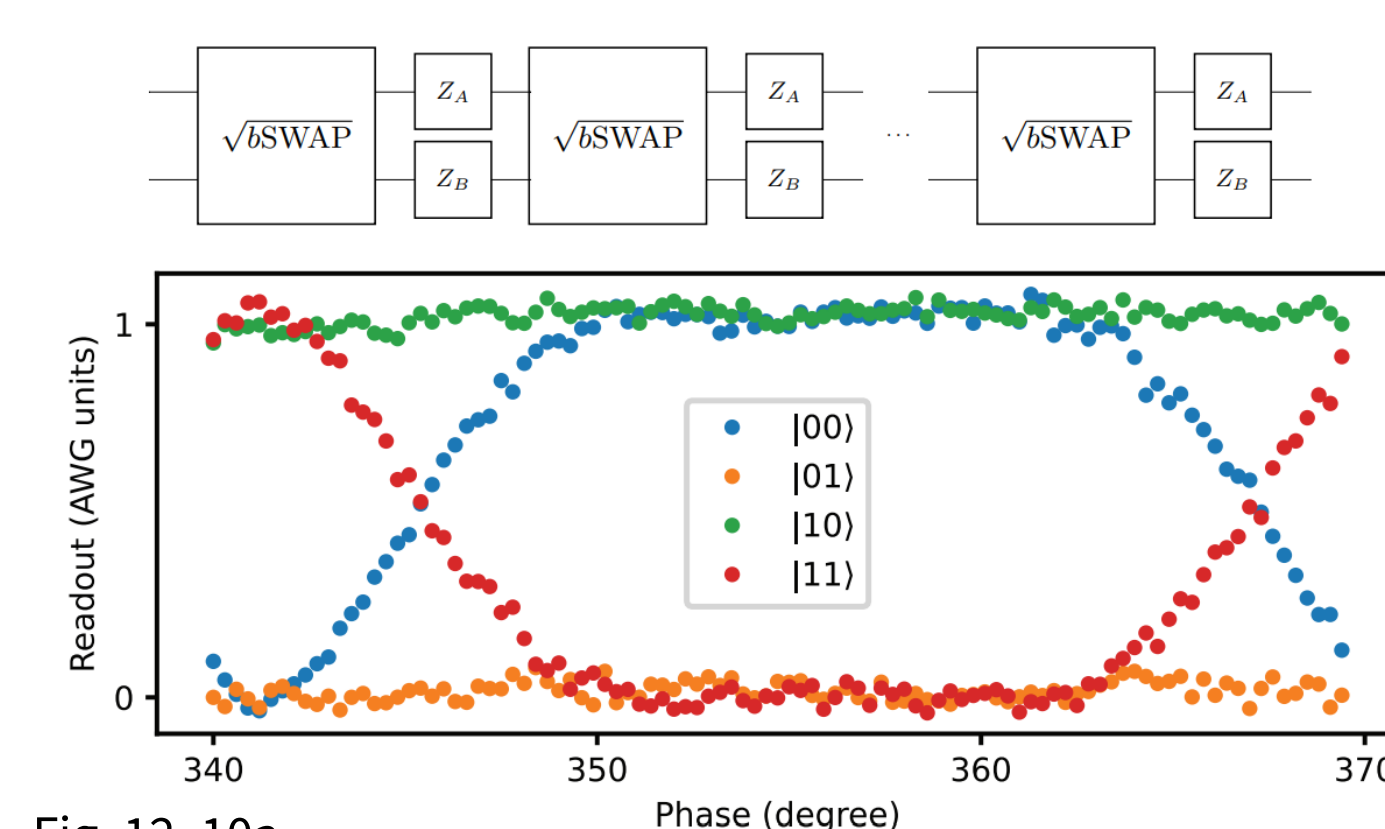


Fig. 12, 10a

Repeatedly playing the pulse amplifies rotation error, allowing phase calibration

- Final pulse parameters:
- $f_{\text{sqb}} = 110.2\text{MHz}$
 - $t_{\text{sqb}} = 101.6\text{ns}$ (5 qubit Larmor periods)
 - $\phi_A = 357^\circ$

To cancel RF crosstalk, play same coupler pulse on $\Phi_{\text{ext}}^A, \Phi_{\text{ext}}^B$ with calibrated A, ϕ

Sweep $A(0.7, 1.5 A_0), \phi(224^\circ, 182^\circ)$ of pulse to observe max oscillation contrast

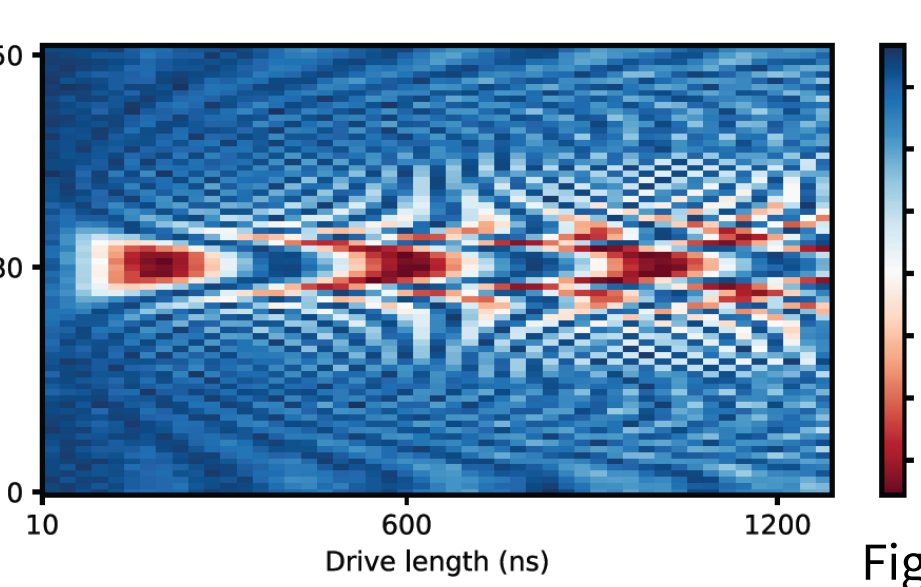


Fig. 9a

Benchmarking Results

Simul. 1Q RB

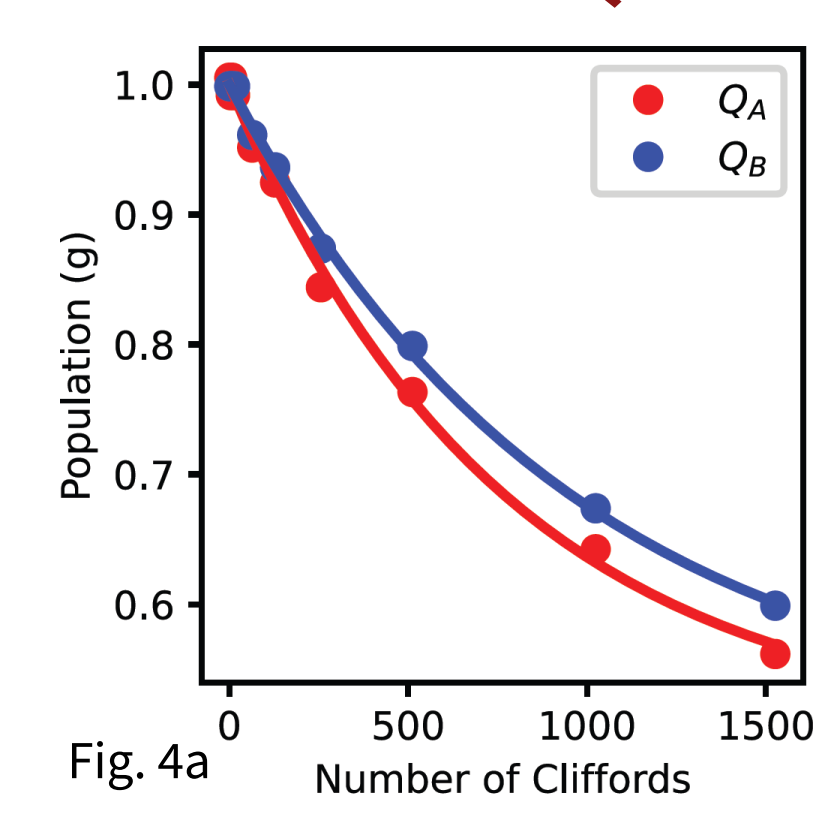


Fig. 4a

DRAG shaping for both 1Q, 2Q gates, optimized via RL

$\sqrt{b\text{SWAP}}$ compiled with 2 virtual Z gates and crosstalk cancellation

2Q XEB

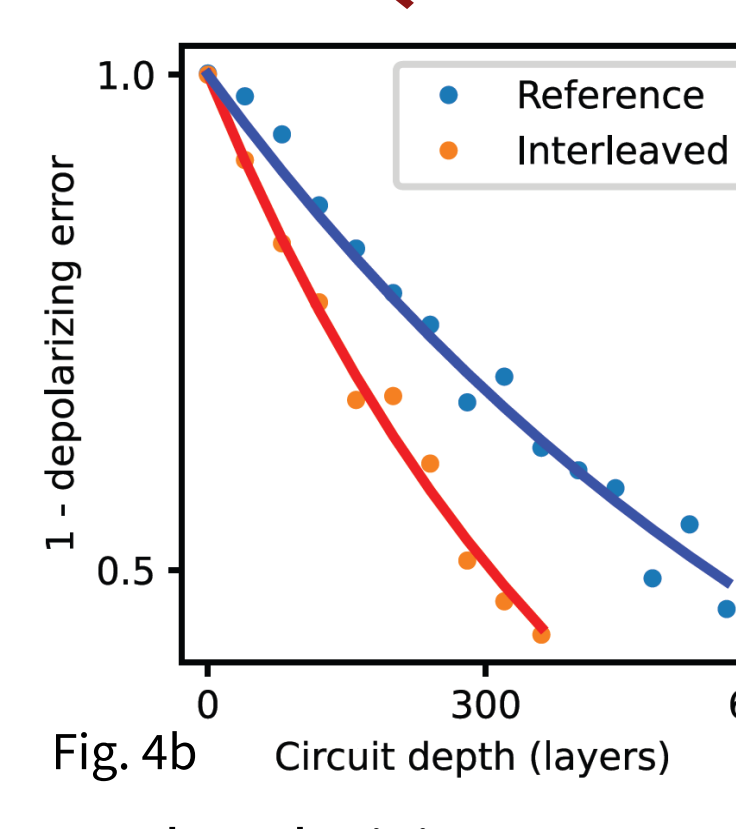


Fig. 4b

Fidelity: qA: 99.94%; qB: 99.95% Gate lengths: qA: 83.3ns; qB: 65.1ns

Avg. depolarizing error: Reference: 1.3×10^{-3} Interleaved: 2.4×10^{-3}

$\sqrt{b\text{SWAP}}$ XEB: $F_{\text{Avg}} = 99.91 \pm 0.02\%$

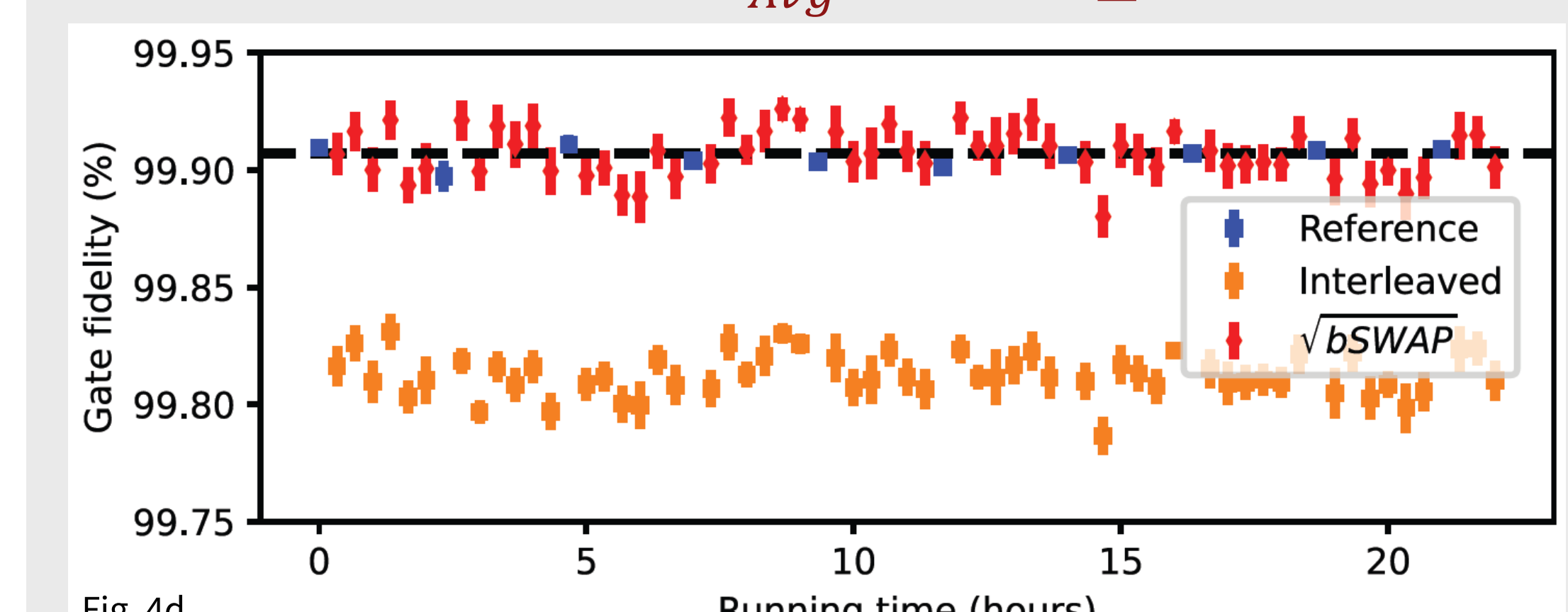


Fig. 4d

Dominant error source: **qubit decoherence**; not limited by RWA/carrier envelope. Full error budget here: Ref App. J

QST

$$\rho = |gg\rangle + i|ee\rangle / \sqrt{2}$$

QPT

$$X = \sqrt{b\text{SWAP}}$$

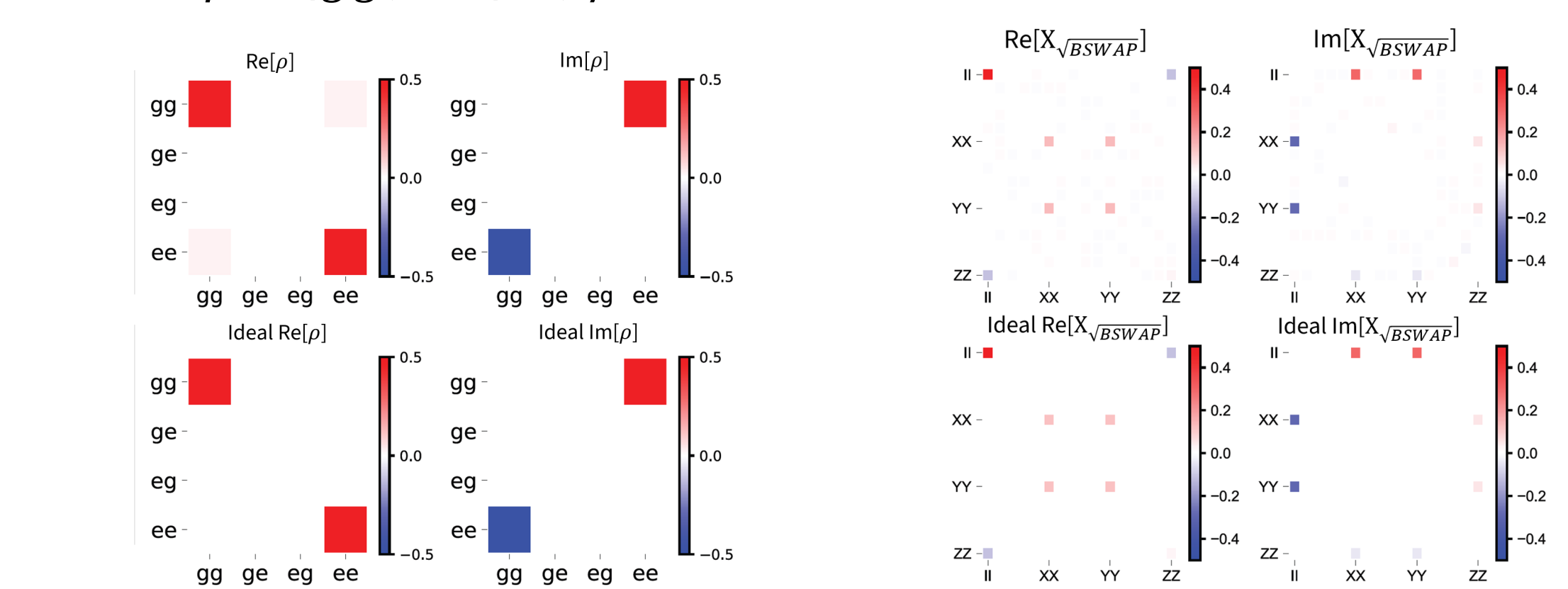


Fig. 11

QST and QPT show fidelity of 95%, limited by SPAM errors

Bibliography

[1] Zhang and Ding, arXiv (2023)

[2] Weiss, PRX (2023)

[3] Stefanazzi, RSI (2022)